

ZmmiR398b negatively regulates maize resistance to sugarcane mosaic virus infection by targeting *ZmCSD2/4/9*

Xinran Gao | Zhichao Du | Kaiqiang Hao | Sijia Zhang | Jian Li | Jinxiu Guo |
Zhiping Wang | Shixue Zhao | Lijun Sang | Mengnan An | Zihao Xia  | Yuanhua Wu 

Liaoning Key Laboratory of Plant Pathology, College of Plant Protection, Shenyang Agricultural University, Shenyang, Liaoning, China

Correspondence

Zihao Xia and Yuanhua Wu, Liaoning Key Laboratory of Plant Pathology, College of Plant Protection, Shenyang Agricultural University, Shenyang, Liaoning 110866, China.

Email: zihao8337@syau.edu.cn and wuyh09@syau.edu.cn

Funding information

China Postdoctoral Science Foundation; National Natural Science Foundation of China

Abstract

MicroRNAs (miRNAs) are widely involved in various biological processes of plants and contribute to plant resistance against various pathogens. In this study, upon sugarcane mosaic virus (SCMV) infection, the accumulation of maize (*Zea mays*) miR398b (*ZmmiR398b*) was significantly reduced in resistant inbred line Chang7-2, while it was increased in susceptible inbred line Mo17. Degradome sequencing analysis coupled with transient co-expression assays revealed that *ZmmiR398b* can target *Cu/Zn-superoxidase dismutase2* (*ZmCSD2*), *ZmCSD4*, and *ZmCSD9* in vivo, of which the expression levels were all upregulated by SCMV infection in Chang7-2 and Mo17. Moreover, overexpressing *ZmmiR398b* (*OE398b*) exhibited increased susceptibility to SCMV infection, probably by increasing reactive oxygen species (ROS) accumulation, which were consistent with *ZmCSD2/4/9*-silenced maize plants. By contrast, silencing *ZmmiR398b* (*STTM398b*) through short tandem target mimic (STTM) technology enhanced maize resistance to SCMV infection and decreased ROS levels. Interestingly, copper (Cu)-gradient hydroponic experiments demonstrated that Cu deficiency promoted SCMV infection while Cu sufficiency inhibited SCMV infection by regulating accumulations of *ZmmiR398b* and *ZmCSD2/4/9* in maize. These results revealed that manipulating the *ZmmiR398b-ZmCSD2/4/9*-ROS module provides a prospective strategy for developing SCMV-tolerant maize varieties.

KEYWORDS

copper, ROS, SCMV, *ZmCSD2/4/9*, *ZmmiR398b*

1 | INTRODUCTION

Maize (*Zea mays*) is an essential food source for humans and animals and a classic model for genetics research. However, a variety of diseases seriously affect the yield and quality of maize

(Liu, Deng, et al., 2020; Mahuku et al., 2015). Among them, maize dwarf mosaic disease (MDMD) is a destructive viral disease that is widespread worldwide; the major causal agent in China is sugarcane mosaic virus (SCMV) (Fan et al., 2003; Li, Liu, et al., 2013; Shi et al., 2005). Sugarcane mosaic virus, a potyvirus,

Xinran Gao and Zhichao Du equally contributed to this work.

This is an open access article under the terms of the [Creative Commons Attribution-NonCommercial-NoDerivs](https://creativecommons.org/licenses/by-nc-nd/4.0/) License, which permits use and distribution in any medium, provided the original work is properly cited, the use is non-commercial and no modifications or adaptations are made.

© 2024 The Authors. *Molecular Plant Pathology* published by British Society for Plant Pathology and John Wiley & Sons Ltd.

is an important and devastating viral pathogen infecting maize, sorghum (*Sorghum vulgare*), sugarcane (*Saccharum sinensis*), and many other *Gramineae* crops (Shukla et al., 1989). Maize plants infected by SCMV exhibit typical leaf mosaic and plant dwarfing symptoms (Jiang & Zhou, 2002), and when coinfecting with maize chlorotic mottle virus (MCMV), it can cause maize lethal necrosis (MLN), resulting in serious losses to maize production (Jiao et al., 2022; Mahuku et al., 2015). Therefore, it is urgent to study the interaction between SCMV and maize plants for uncovering the underlying molecular mechanisms and breeding resistant maize varieties.

Plant miRNAs are a class of 20–24 nucleotide noncoding RNAs that function by inhibiting the expression of messenger RNAs (mRNAs) via degradation or translational repression (Padmanabhan et al., 2009; Wang et al., 2019). A growing body of research suggests that miRNAs could regulate plant development (Dong et al., 2022). For instance, miR172 participates in the floral development and flowering time in maize, *Arabidopsis thaliana*, soybean, rice, and barley (Chen, 2004; Tang & Chu, 2017). In addition, miR164 and its target gene *NAC1* can regulate the formation of lateral roots in maize and *Arabidopsis* (Guo et al., 2005; Li et al., 2012). Many miRNAs have been shown to play central roles in plant adaptation to various stresses (Chaudhary et al., 2021). The overexpression of miR160a modulates plant defence against *Magnaporthe oryzae* accompanied by a decrease in the expression of three auxin response factors (Li et al., 2014). Upon rice stripe virus (RSV) infection, the upregulated AGO18 preferentially binds to miR528, resulting in elevated activity of its target L-ascorbate oxidase (AO), higher basal reactive oxygen species (ROS) accumulation, and enhanced antiviral defence (Wu et al., 2017). It has been reported that the development of rice disease symptoms caused by rice ragged stunt virus (RRSV) infection is related to the induction of miR319 to inhibit the jasmonic acid (JA)-mediated host defence (Zhang et al., 2016).

miR398 is evolutionarily well conserved in many plants and can suppress the expression of superoxide dismutase (SOD) family members to play vital roles in response to biotic and abiotic stresses (Guan et al., 2013; Xin et al., 2010; Yu et al., 2012). Winter wheat miR398 downregulates its target gene *Cu/Zn-SOD1* (*CSD1*) to regulate low-temperature tolerance, and a lncRNA indirectly regulates the expression of *CSD1* by competitively binding miR398, thereby affecting the cold resistance (Lu et al., 2020). Tomato miR398a is involved in response to drought stress (Candar-Cakir et al., 2016). miR398 and *CSDs* can also regulate plant disease resistance against pathogens. In barley, miR398 represses the expression of target gene *SOD1*, affecting the defence against powdery mildew (Xu et al., 2014). Previous research has shown that rice miR398b overexpression lines (OX398b) have enhanced resistance against *M. oryzae*, which is associated with decreased expression levels of *CSD1*, *CSD2*, *SODX*, and *CCSD* (Li et al., 2014). In addition, lethal systemic necrosis in potato spindle tuber viroid-infected *DCL2/4*-knockdown transgenic *Solanum lycopersicum* is

accompanied by miR398 upregulation and ROS overproduction (Suzuki et al., 2019).

Superoxide radicals (O_2^-) and hydrogen peroxide (H_2O_2), as two species of ROS, play indispensable roles in plant development and stress responses (Jajic et al., 2015; Mhamdi & Van Breusegem, 2018). The synthesis and homeostasis of intracellular ROS are strictly regulated by the NADPH oxidase, SOD, catalase (CAT), and ascorbate peroxidase (APX) in plants. Researchers successively found three kinds of SODs with different metal cofactors, including *CSD*, manganese SOD (*SOD-Mn*), and iron SOD (*SOD-Fe*) (Mittler, 2002). Acting as synthetases, SODs can convert O_2^- into H_2O_2 (Asada, 2006). It has been reported that miR398 regulates oxidative stress response by inhibiting the expression of *CSD1* and *CSD2* in *Arabidopsis* (Sunkar et al., 2006). Previous studies have shown that H_2O_2 could regulate plant tolerance against various stresses (Saxena et al., 2016). Overexpression of AO increased H_2O_2 content, thereby enhancing rice resistance to RSV infection (Wu et al., 2017). In plants, ROS-mediated stress resistance is regulated by enzyme systems related to ROS homeostasis, which seems to be tuned by certain miRNAs (Baldrich & San Segundo, 2016). For instance, in *Nicotiana benthamiana*, miR398 and its target *NbCSD2* regulate resistance against bamboo mosaic virus (BaMV) infection by mediating ROS content (Lin et al., 2022).

Previous studies have demonstrated the role of miR398 and its targets in copper (Cu) homeostasis (Pilon, 2017). In grapevine, miR398 mediates responses to Cu stress by regulating the expression of its target genes *VvCSD1* and *VvCSD2* (Leng et al., 2017). *Cca-miR398* increases copper sulphate stress sensitivity via the regulation of *CSD* mRNA transcription levels in transgenic *A. thaliana* (Sun et al., 2020). miR398 was reported to target *CSD1* and *CSD2* that use copper as cofactors and regulate tolerance to Cu stress in *A. thaliana* (Yamasaki et al., 2007). Elevating Cu content in vitro or in vivo could promote rice antiviral defence by regulating SPL9-miR528-AO-mediated ROS signalling (Yao et al., 2022). However, the molecular mechanisms underlying how Cu coordination with the ZmmiR398b-ZmCSD2/4/9-ROS module regulates maize antiviral defence responses are unclear.

In the present study, the expression of ZmmiR398b was downregulated in resistant maize inbred line Chang7-2 while it was upregulated in susceptible maize inbred line Mo17 at 10 days post-inoculation (dpi) with SCMV infection. To further analyse the antiviral function of ZmmiR398b, we obtained overexpressing (OE398b) and silenced ZmmiR398b (STTM398b) transgenic maize lines. In addition, the virus-induced gene silencing (VIGS) technique was used to silence three target genes, *ZmCSD2*, *ZmCSD4*, and *ZmCSD9*, of ZmmiR398b simultaneously. Through determining the content of ROS, we found that ZmmiR398b negatively regulated maize resistance to SCMV infection by targeting *ZmCSD2/4/9* and probably modulating ROS accumulation. Moreover, hydroponic experiments were carried out to study the effect of Cu deficiency or sufficiency on SCMV infection in maize. Our results demonstrated that the

ZmmiR398b-ZmCSD2/4/9-ROS module participated in maize resistance to SCMV infection.

2 | RESULTS

2.1 | The expression levels of ZmmiR398b and its target genes were affected by SCMV infection

To identify SCMV-responsive miRNAs, small RNA sequencing was performed using SCMV-infected resistant (Chang7-2) and susceptible (Mo17) maize inbred lines in our previous report, and the relative expression levels of ZmmiR398b in different resistant and susceptible maize inbred lines are shown in Table S2. The results indicated that upon SCMV infection, ZmmiR398b showed opposite expression trends in different maize inbred lines (Gao et al., 2023). Here, the expression pattern of ZmmiR398b was further verified in Chang7-2 and Mo17 by reverse transcription-quantitative PCR (RT-qPCR). As revealed by small RNA sequencing data, the expression of ZmmiR398b was significantly suppressed by SCMV infection in Chang7-2 (Figure 1a), while it was significantly upregulated in Mo17 at 10 dpi (Figure 1a). ZmmiR398b accumulated at a lower level in Mo17 than in Chang7-2 without SCMV infection (Figure 1a). It is interesting that upon SCMV infection, ZmmiR398b accumulated at a higher level in Mo17 compared with that in Chang7-2 (Figure 1a), indicating that ZmmiR398b may be involved in maize resistance to SCMV infection in different maize lines. In our previous study, a degradome library was constructed and sequenced to identify targets of maize miRNAs (Gao et al., 2023). The results revealed that ZmmiR398b could potentially cleave Zm00001d022505_T003 (ZmCSD2), Zm00001d029170_T003 (ZmCSD4), and Zm00001d047479_T003 (ZmCSD9) (Figure S1). Interestingly, compared with mock treatment, the expression levels of ZmCSD2,

ZmCSD4, and ZmCSD9 were all significantly upregulated in SCMV-infected Chang7-2 and Mo17 (Figure 1b,c).

2.2 | ZmmiR398b can target ZmCSD2, ZmCSD4, and ZmCSD9 in *N. benthamiana* through transient co-expression analysis

Although CSDs have been shown to be targeted by miR398 in many plants (Leng et al., 2017; Sunkar et al., 2006), whether miR398 targets CSDs in maize remains to be determined. To test the targeting action of ZmmiR398b on ZmCSD2, ZmCSD4, and ZmCSD9, transient co-expression analyses in *N. benthamiana* leaves were performed. The sequence alignments of ZmmiR398b with ZmCSD2, ZmCSD4, and ZmCSD9 target sites and mutated target sites are shown in Figure S2. The transient co-expression results showed that the green fluorescence intensity from pGD-CSD2_{ts}-green fluorescent protein (GFP), pGD-CSD4_{ts}-GFP, and pGD-CSD9_{ts}-GFP was gradually reduced with the increased concentration of pGD-miR398b (Figure 2a,c,e). However, the green fluorescence intensity was not changed when pGD-CSD2_{ts}-GFP, pGD-CSD4_{ts}-GFP, or pGD-CSD9_{ts}-GFP was co-infiltrated with pGD-miR159a, or pGD-CSD2_{mts}-GFP, pGD-CSD4_{mts}-GFP, or pGD-CSD9_{mts}-GFP was co-infiltrated with different concentrations of pGD-miR398b (Figure 2a,c,e). The GFP RNA (Figure S3a-c) and protein levels (Figure 2b,d,f) were consistent with the fluorescence intensity. These results indicated that ZmCSD2, ZmCSD4, and ZmCSD9 could be targeted by ZmmiR398b.

2.3 | ZmmiR398b negatively regulated maize resistance to SCMV infection

To further explore the roles of ZmmiR398b in maize resistance to SCMV infection, we generated stably overexpressing (OE398b) and

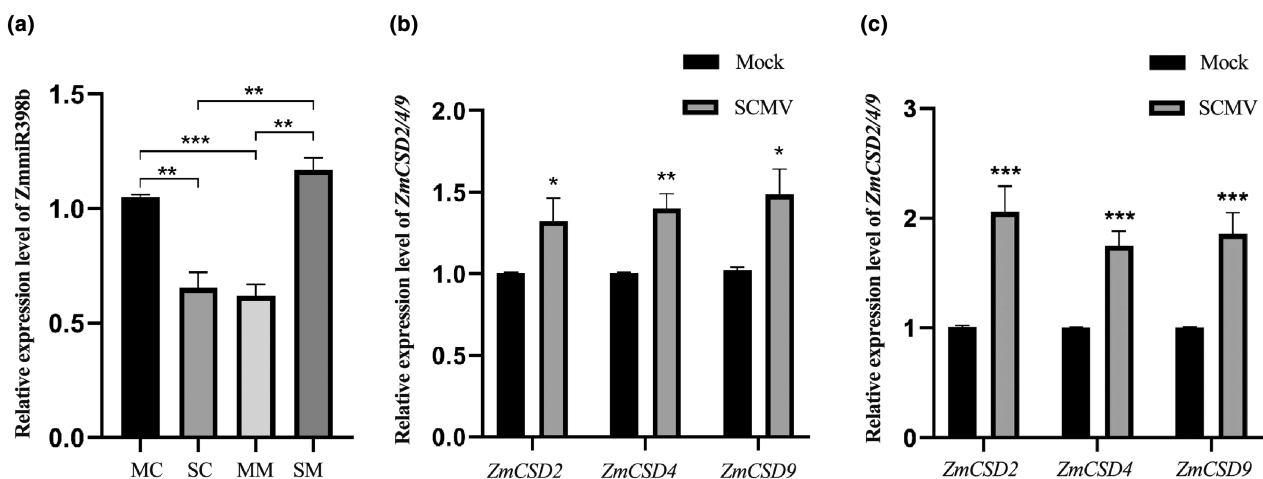
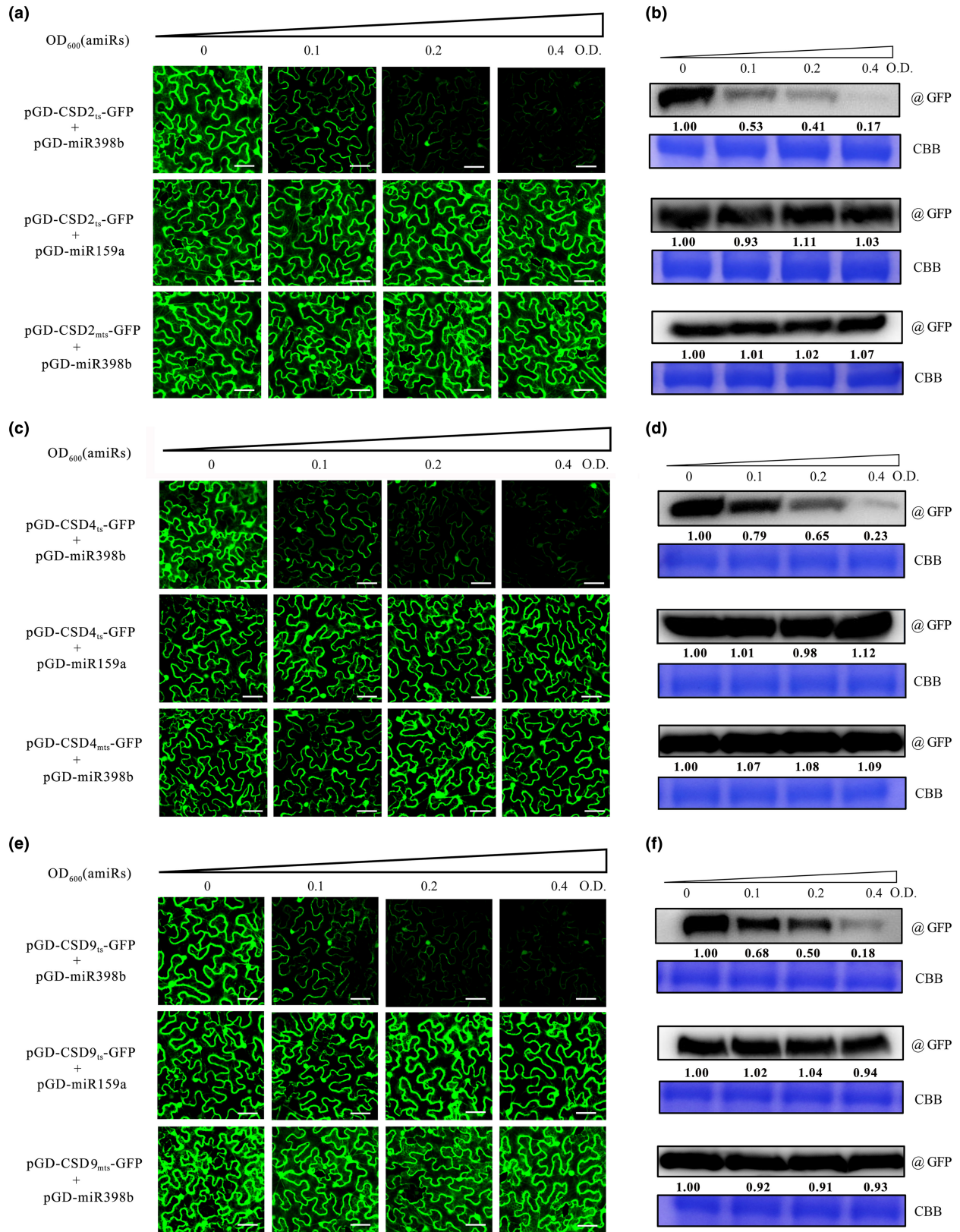


FIGURE 1 The expression levels of ZmmiR398b and its target genes. (a) The expression level of ZmmiR398b in Chang7-2 and Mo17. (b) The expression levels of ZmCSD2, ZmCSD4, and ZmCSD9 in Chang7-2. (c) The expression levels of ZmCSD2, ZmCSD4, and ZmCSD9 in Mo17. All data are expressed as the means \pm SD of three independent experiments. MC and SC represent Chang7-2 inoculated with phosphate buffer and sugarcane mosaic virus (SCMV), respectively; MM and SM represent Mo17 inoculated with phosphate buffer and SCMV, respectively. * $p < 0.05$, ** $p < 0.01$, *** $p < 0.001$.



silenced (STTM398b) ZmmiR398b transgenic maize lines. The PCR was used to amplify the bialaphos resistance gene (*bar*) to verify the transgenic lines (Figure S4), and three lines of OE398b and STTM398b were selected for further analyses. Compared with that in wild-type (WT) plants, the expression level of ZmmiR398b was

increased by 3.5–3.9-fold in OE398b-5, OE398b-10, and OE398b-14 lines (Figure 3a), whereas it was decreased by approximately 60% in STTM398b-1, STTM398b-2, and STTM398b-6 lines (Figure 3a). The expression levels of ZmmiR398b target genes *ZmCSD2*, *ZmCSD4*, and *ZmCSD9* were significantly decreased by approximately 55%

FIGURE 2 ZmmiR398b targeted *ZmCSD2*, *ZmCSD4*, and *ZmCSD9* in *Nicotiana benthamiana*. (a) Samples of agrobacteria harbouring the constructs expressing pGD-CSD2_{ts}-GFP with pGD-miR398b; pGD-CSD2_{ts}-GFP with pGD-miR159a; or pGD-CSD2_{mts}-GFP with pGD-miR398b were mixed with a different ratio for co-expression in *N. benthamiana*. (c) Samples of agrobacteria harbouring the constructs pGD-CSD4_{ts}-GFP with pGD-miR398b; pGD-CSD4_{ts}-GFP with pGD-miR159a; or pGD-CSD4_{mts}-GFP with pGD-miR398b were mixed with a different ratio for co-expression in *N. benthamiana*. (e) Samples of agrobacteria harbouring the constructs pGD-CSD9_{ts}-GFP with pGD-miR398b; pGD-CSD9_{ts}-GFP with pGD-miR159a; or pGD-CSD9_{mts}-GFP with pGD-miR398b were mixed with a different ratio for co-expression in *N. benthamiana*. The confocal images were taken at 48 h after infiltration. (b, d, f) The protein levels of GFP in different treatments were detected by anti-GFP antibodies. CBB, Coomassie brilliant blue. Scale bar = 20 μm.

in OE398b plants (Figure 3b), whereas they were significantly increased by approximately 2.4-fold in STTM398b plants (Figure 3b). Compared with WT plants, SCMV infection caused more severe mosaic symptoms on OE398b plants, whereas it only produced very mild mosaic symptoms on STTM398b plants at 6 dpi (Figure 3c). Moreover, in OE398b-5, OE398b-10, and OE398b-14 lines, the accumulation of SCMV genomic RNA and coat protein (CP) at 6 dpi was increased by 4.9–5.3-fold and 1.7–1.9-fold of that in WT plants, respectively (Figure 3d,e). By contrast, the accumulation of SCMV genomic RNA and CP at 6 dpi in the STTM398b-1, STTM398b-2, and STTM398b-6 lines was decreased by approximately 50% and 70% of that in WT plants, respectively (Figure 3d,e). To determine whether the ROS regulated by *ZmCSDs* were involved in resistance to SCMV infection, the content of O₂⁻ and H₂O₂ in SCMV-infected OE398b, STTM398b, and WT maize plants was measured by nitroblue tetrazolium (NBT) and 3,3'-diaminobenzidine (DAB) staining assays, respectively. The results revealed that the accumulation of both O₂⁻ and H₂O₂ in OE398b lines was greater, while it was less in STTM398b lines, than that in WT plants (Figure 3f,g). These results demonstrated that ZmmiR398b negatively regulated maize resistance against SCMV infection probably by modulating ROS accumulation.

2.4 | Knockdown of *ZmCSD2*, *ZmCSD4*, and *ZmCSD9* promoted SCMV infection in maize

To investigate the function of *ZmCSD2*, *ZmCSD4*, and *ZmCSD9* against SCMV infection, we simultaneously silenced them using cucumber mosaic virus (CMV)-based virus-induced gene silencing (VIGS) assays. Upon SCMV infection, the symptoms on *ZmCSD2/4/9*-knockdown plants (CMV-*ZmCSD2/4/9*) were more severe than that on control plants (CMV-GFP₂₅₄) (Figure 4a). At 7 dpi, the second systemically infected leaves were harvested to determine the *ZmCSD2/4/9* silencing efficiency, the accumulation of SCMV, and the content of O₂⁻ and H₂O₂. The RT-qPCR results revealed that compared with CMV-GFP₂₅₄ plants, the expression levels of *ZmCSD2*, *ZmCSD4*, and *ZmCSD9* were decreased by 44%, 35%, and 52% in CMV-*ZmCSD2/4/9* plants, respectively (Figure 4b). In CMV-*ZmCSD2/4/9* plants, the accumulation of SCMV genomic RNA and CP was increased by 3.1-fold and 1.6-fold, respectively, compared to that in CMV-GFP₂₅₄ plants (Figure 4c,d). Moreover, more O₂⁻ and H₂O₂ accumulated in CMV-*ZmCSD2/4/9* plants than in CMV-GFP₂₅₄ plants (Figure 4e). These results indicated that silencing the target genes of ZmmiR398b, *ZmCSD2*, *ZmCSD4*, and

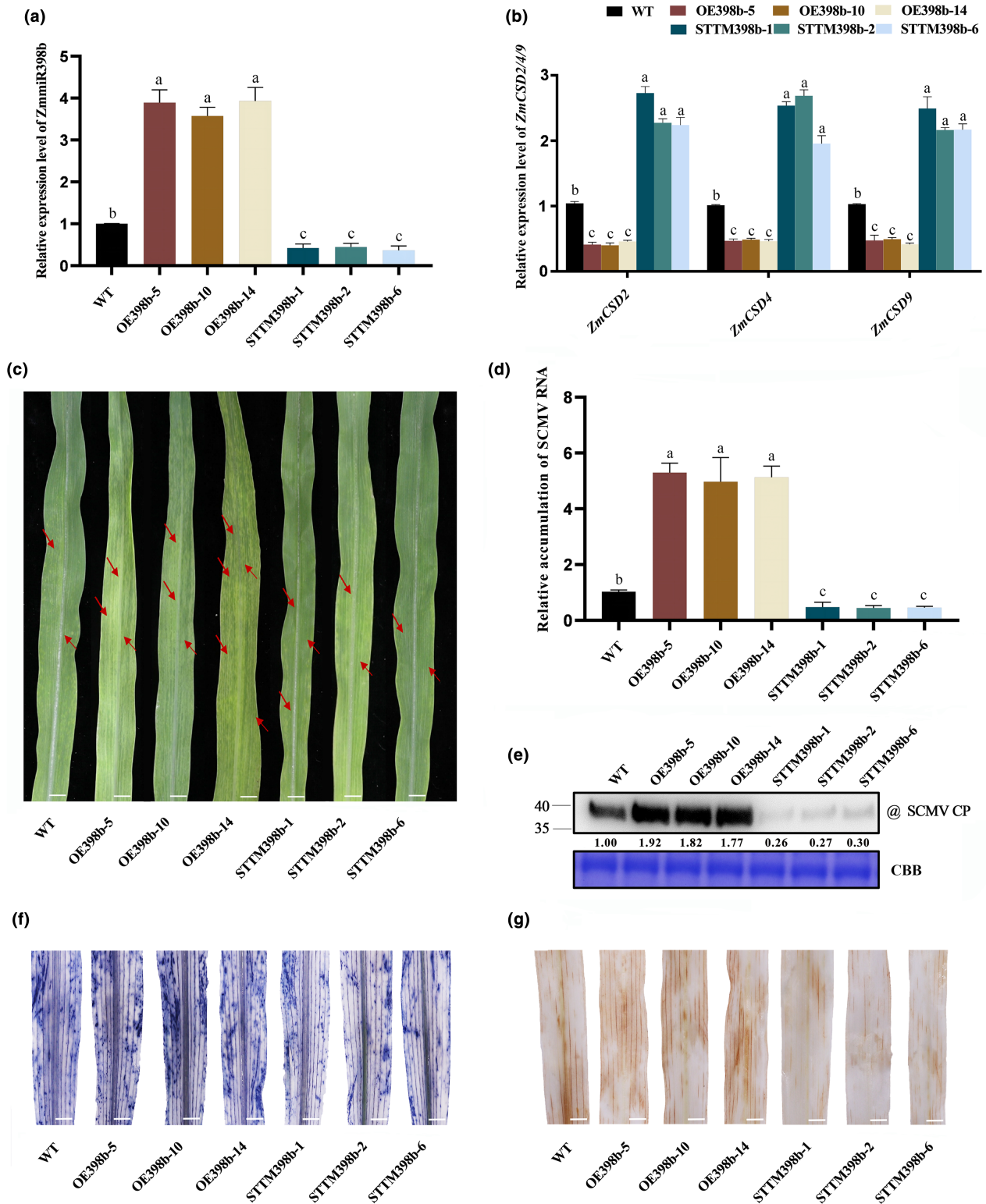
ZmCSD9, promoted SCMV infection in maize, probably by regulating ROS content.

2.5 | Cu sufficiency inhibited SCMV infection in maize

miR398 is known to be involved in the regulation of Cu homeostasis (Pilon, 2017). To explore the roles of Cu in resistance to SCMV infection, maize seedlings were cultivated in Cu-gradient nutrient solution. The results indicated that upon SCMV infection, the first systemically infected leaves of 50 μg/L CuSO₄·5H₂O (sufficiency, Cu²)-treated maize plants showed weaker mosaic symptoms than that of 25 μg/L CuSO₄·5H₂O (normal, Cu¹)-treated maize plants at 7 dpi. Compared with the Cu² and Cu¹ treatments, the first systemically infected leaves of 0 μg/L CuSO₄·5H₂O (deficiency, Cu⁰)-treated maize plants exhibited more severe mosaic symptoms at 7 dpi (Figure 5a). Compared with the plants treated by Cu¹, Cu⁰ treatment significantly upregulated the expression of ZmmiR398b (Figure 5b), whereas it reduced the expression of *ZmCSD2*, *ZmCSD4*, and *ZmCSD9* at different stages of SCMV infection (Figure 5c–e). In contrast, Cu² treatment significantly reduced the expression of ZmmiR398b (Figure 5b), whereas it upregulated the expression of *ZmCSD2*, *ZmCSD4*, and *ZmCSD9* (Figure 5c–e). Moreover, we assessed the accumulation of SCMV genomic RNA and CP using RT-qPCR and western blotting at 3, 5, 7, and 9 dpi, respectively. The results indicated that Cu⁰ increased the accumulation of SCMV genomic RNA and CP, while Cu² decreased viral accumulation at different periods of SCMV infection (Figure 5f,g). These results demonstrated that Cu sufficiency could inhibit SCMV infection and significantly relieve the mosaic symptoms on maize plants, probably by modulating the expression of the ZmmiR398b regulatory pathway.

3 | DISCUSSION

Cultivating virus-resistant varieties is the most reliable method for controlling plant virus disease (Redinbaugh & Stewart, 2018). miRNA-mediated gene silencing plays an important role in plant antiviral responses (Liu et al., 2022; Xia et al., 2018). miR398 has been identified to regulate plant resistance by suppressing the expression of CSD genes (Lin et al., 2022; Wang et al., 2019). Different pathogens can manipulate expression levels of miR398, thereby creating a better environment for their infection. For example, BaMV infection elevates the expression of miR398, and the accumulation of BaMV



is regulated positively by miR398 in *N. benthamiana* (Lin et al., 2022). In contrast, in beet necrotic yellow vein virus (BNYVV)-infected *N. benthamiana*, increased miR398 is able to activate the immune system and restrict BNYVV infection (Liu, Fan, et al., 2020). In this study, we found that ZmmiR398b expression was reduced in resistant maize inbred line Chang7-2, while it was increased in susceptible maize inbred line Mo17 after SCMV infection (Figure 1a). Moreover,

SCMV infection was promoted by overexpressing ZmmiR398b compared with that of WT plants, while it was inhibited in silenced ZmmiR398b maize plants (Figure 3c-e), indicating that ZmmiR398b plays important roles in negatively regulating maize resistance to SCMV infection.

To date, CSDs have been demonstrated to function as conserved targets of miR398 in *Arabidopsis*, rice, and *N. benthamiana*

FIGURE 3 ZmmiR398b negatively regulated maize resistance to sugarcane mosaic virus (SCMV) infection. (a) Relative expression levels of ZmmiR398b were determined by reverse transcription-quantitative PCR (RT-qPCR), and the expression level of *U6* was used as an internal control. WT, wild-type; OE, ZmmiR398b overexpressing lines; STTM, ZmmiR398b silenced lines. (b) Relative expression levels of *ZmCSD2/4/9* were determined by RT-qPCR, and the expression level of *ZmUBI* was used as an internal control. (c) The symptoms on the first systemically infected leaves in control (WT) and ZmmiR398b transgenic maize plants at 6 days post-inoculation (dpi). Scale bars = 1 cm. (d) The accumulation of SCMV genomic RNA in control plants and ZmmiR398b transgenic maize plants determined by RT-qPCR. (e) The expression of SCMV coat protein (CP) in control plants and ZmmiR398b transgenic maize plants by western blot analyses. CBB, Coomassie brilliant blue staining of loading control. (f) Nitroblue tetrazolium (NBT) staining of control plant and ZmmiR398b transgenic maize plant leaves for O_2^- at 6 dpi. Scale bars = 1 cm. (g) 3,3'-diaminobenzidine (DAB) staining of control plant and ZmmiR398b transgenic maize plant leaves for H_2O_2 at 6 dpi. Scale bars = 1 cm. The results are presented as the mean \pm SD from three independent experiments. Statistical significance between two different treatments was determined using one-way analysis of variance followed by Duncan's multiple comparison test. Different lowercase letters indicate statistically significant differences between treatments ($p < 0.05$). The relative densities of each band detected in western blotting were analysed by the ImageJ software.

(Li et al., 2019; Lin et al., 2022; Sunkar & Zhu, 2004). By means of transient co-expression assays in *N. benthamiana*, we clearly proved that ZmmiR398b could target the *ZmCSD2*, *ZmCSD4*, and *ZmCSD9* genes (Figure 2). SCMV infection significantly increased the abundance of *ZmCSD2/4/9* transcripts in both Chang7-2 and Mo17, although the expression of ZmmiR398b was upregulated in SCMV-infected Mo17 plants (Figure 1b,c). Previous studies have shown that the accumulation of miR398 and *NbCSD* transcription was increased simultaneously in potato virus X (PVX)-, potato virus Y (PVY)-, or BaMV-infected *N. benthamiana* plants (Lin et al., 2022; Pacheco et al., 2012). HC-Pro, an RNA silencing suppressor encoded by SCMV, suppresses RNA silencing induced by sense RNA and dsRNA (Zhang et al., 2008). It has been reported that HC-Pro could interfere with miRNA to function and increase miRNA accumulation (Kasschau et al., 2003), and the induction of both miRNAs and their targets by several potyviruses, such as SCMV or turnip mosaic virus, has been found (Cui et al., 2020; Xia et al., 2018). Therefore, amounts of HC-Pro accompanied by SCMV infection accumulated in maize susceptible inbred line Mo17 that interfered with miRNAs, resulting in upregulated expression of both ZmmiR398b and *ZmCSD2/4/9*. Moreover, the expression levels of ZmmiR398b target genes, *ZmCSD2/4/9*, were upregulated to activate the immune system and defend against SCMV infection.

ROS play multifaceted signalling functions in mediating the establishment of various responses (Waszczak et al., 2018). SODs are a group of antioxidant enzymes responsible for ROS clearance (Gill & Tuteja, 2010) and catalyse the conversion of O_2^- into H_2O_2 , which acts as a signal molecule to trigger resistance to various biotic and abiotic stresses (Kaur et al., 2016; Quan et al., 2008). However, excessive H_2O_2 will lead to oxidative stress and result in programmed cell death (PCD), which is harmful to plant development (Quan et al., 2008). Studies have shown that some enzymes, such as APX and CAT, are involved in regulating the homeostasis of ROS, which catalyses the reduction of H_2O_2 into H_2O and O_2 (Racchi, 2013). It has been reported that the ROS levels were positively related to viral infections and disease symptoms. The developmental symptoms of cucumber mosaic virus (CMV)-infected *Nicotiana tabacum* plants were related to the levels of H_2O_2 , superoxide, and CMV-encoded coat protein (Lei et al., 2016). The latest research demonstrated that silencing *ZmPAO1*, which is involved in producing H_2O_2 , or treatment with an inhibitor of PAO

activity, inhibited MCMV infection in maize (Liu et al., 2022). Similarly, MCMV-encoded p31 can block ZmCATs and inhibit their ability to clear H_2O_2 , promoting MCMV accumulation and disease symptom development in maize (Jiao et al., 2021). Moreover, in *N. benthamiana*, overexpression of *NbLTP1* activated pathogenesis-related (PR) genes and reduced oxidative damage and ROS accumulation, thereby increasing resistance to tobacco mosaic virus (Zhu et al., 2023). In uninfected cells, PrCSD2 is transported into chloroplasts and catalyses the conversion of O_2^- into H_2O_2 , which is catalysed into water by APX; however, BaMV infection induces PrCSD2 cytosolic retention, which cannot enter the chloroplast to function. Moreover, H_2O_2 accumulation may lead to BaMV-induced chlorotic symptoms (Lin et al., 2022). In addition, the manifestation of mosaic symptoms in SCMV-infected maize leaves is accompanied by elevated levels of H_2O_2 (Jiang et al., 2022). A recent report showed that ZmCATs could enhance SCMV replication by mitigating cellular oxidative damage caused by excessive H_2O_2 (Tian et al., 2024). In the present study, OE398b transgenic lines showed decreased resistance to SCMV and accumulated more ROS than WT plants to accelerate severe mosaic symptoms, which is consistent with the results of knockdown of ZmmiR398b target genes *ZmCSD2/4/9* (Figures 3f,g and 4e). In contrast, STTM398b transgenic maize lines showed enhanced resistance to SCMV and accumulated lower amounts of ROS to alleviate mosaic symptoms (Figure 3f,g). It has been reported that the activities of SOD, CAT, GPOD, and APX in *sly-MIR398b#OE* plants were decreased compared with *pBI121#OE* control plants (Liu et al., 2023). We speculate that ZmmiR398b not only regulates the expression of CSD, but also affects the expression of APX related to H_2O_2 elimination, thus unifying the changes in O_2^- and H_2O_2 . Our research proves that the ZmmiR398b-ZmCSDs regulatory module can manage ROS to regulate resistance to SCMV, which expands our understanding of ZmmiR398b-mediated regulation of *ZmCSD2/4/9* on plant stress responses.

Cu is an essential micronutrient for plants and plays an important role in respiration, photosynthesis, ethylene perception, cell wall remodelling, and ROS metabolism (Burkhead et al., 2009). Cu deficiency has adverse effects on plant growth, such as decreased growth rate, distortion, or whitening of young leaves, as well as damage to the apical meristem; excessive Cu is also toxic, causing production of free radicals, resulting in stunted growth and reduced crop yields (Burkhead et al., 2009; Yamasaki et al., 2008). It

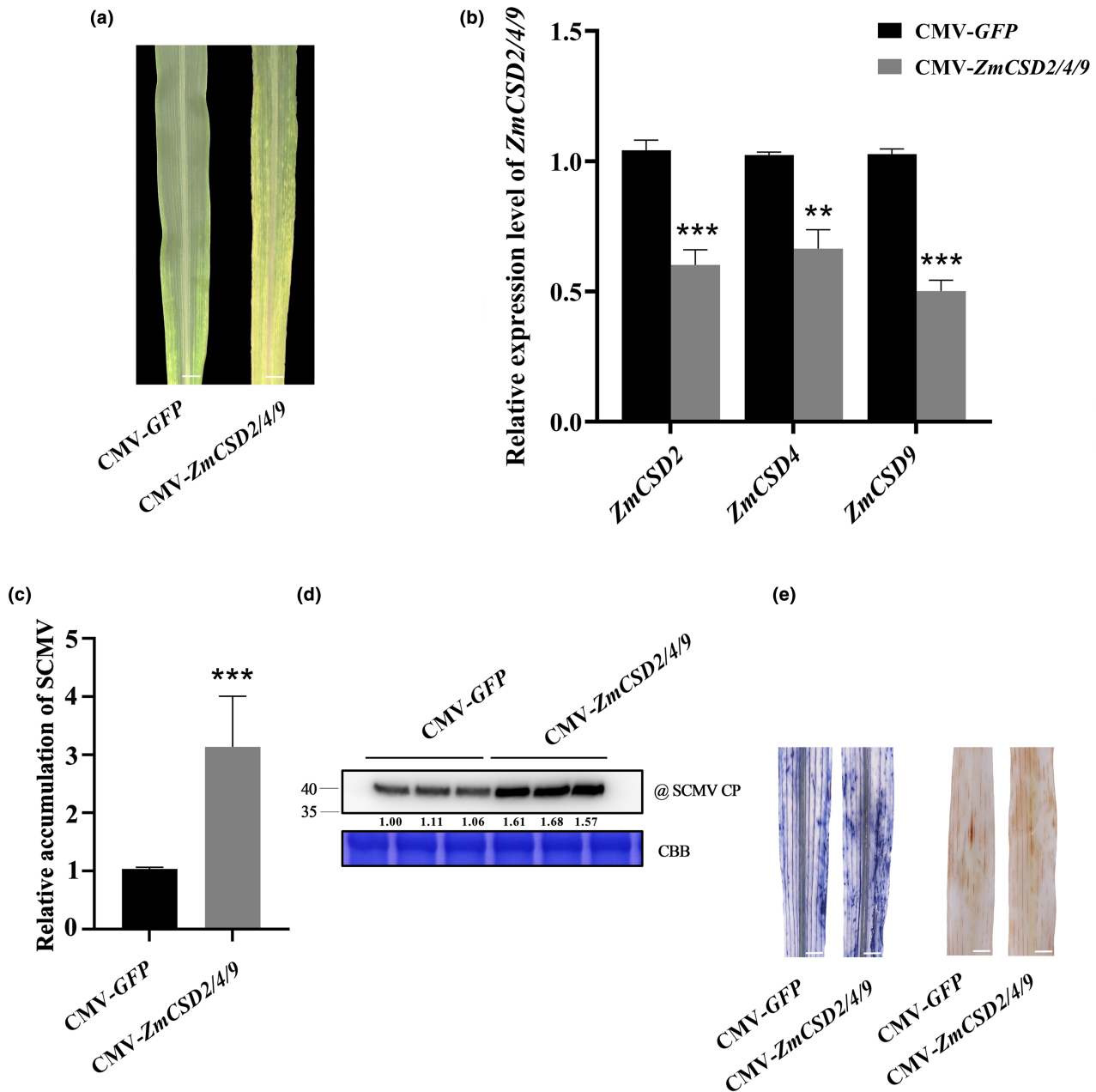


FIGURE 4 Silencing *ZmCSD2*, *ZmCSD4*, and *ZmCSD9* promoted sugarcane mosaic virus (SCMV) infection in maize. (a) The symptoms on SCMV-infected maize leaves of *ZmCSD2/4/9*-silenced plants and controls at 7 days post-inoculation (dpi). Scale bars = 1 cm. (b) Silencing efficiencies of *ZmCSD2*, *ZmCSD4*, and *ZmCSD9*. (c) The accumulation of SCMV genomic RNA in *ZmCSD2/4/9*-silenced maize plants and controls at 7 dpi determined by reverse transcription-quantitative PCR. (d) The expression of SCMV coat protein (CP) in *ZmCSD2/4/9*-silenced maize plants and controls at 7 dpi by western blot analysis. CBB, Coomassie brilliant blue loading control. (e) Nitroblue tetrazolium (NBT) and 3,3'-diaminobenzidine (DAB) stainings of *ZmCSD2/4/9*-silenced maize plants and controls infected with SCMV at 7 dpi for O_2^- and H_2O_2 detection. Scale bars = 1 cm. The results were statistically analysed using two-tailed Student's *t* test. All data are expressed as the means \pm SD of three independent experiments. ***p* < 0.01, ****p* < 0.0001.

has been reported that appropriately elevating Cu content in vitro or in vivo could promote rice antiviral defence by regulating SPL9-miR528-AO-mediated ROS signalling (Yao et al., 2022). The main function of CSDs is to maintain the homeostasis of Cu and intracellular ROS. In plants, several conserved copper-responsive miRNAs, such as miR398, miR397, miR408, and miR857, play crucial roles in regulating Cu homeostasis (Burkhead et al., 2009; Yamasaki

et al., 2007). Interestingly, these miRNAs mainly target CSDs and several laccases, which encode copper-containing proteins. Under Cu deprivation, miRNAs were increased and downregulated the expression of target genes, suggesting that copper-responsive miRNAs can silence CSDs and laccases to save Cu for more essential proteins (Abdel-Ghany & Pilon, 2008; Yamasaki et al., 2008). miR398 has been reported to respond to Cu stress in plants by

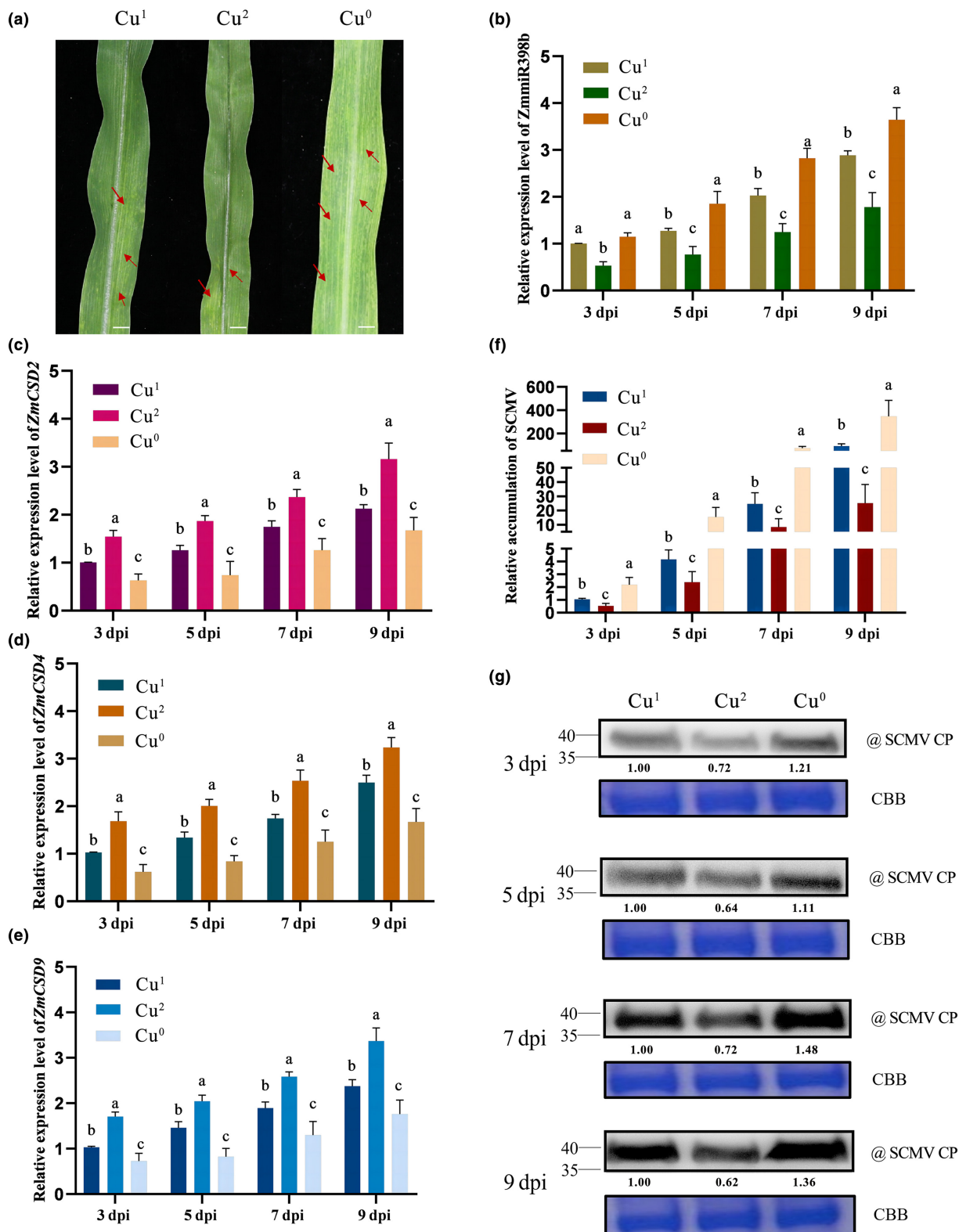


FIGURE 5 Copper (Cu) sufficiency inhibited sugarcane mosaic virus (SCMV) infection in maize. (a) The symptoms of the first systemically infected leaves after SCMV infection in Hoagland's nutrient solution with different Cu concentrations at 7 days post-inoculation (dpi). Cu^0 , deficiency, 0 $\mu\text{g/L}$ $\text{CuSO}_4 \cdot 5\text{H}_2\text{O}$; Cu^1 , normal, 25 $\mu\text{g/L}$ $\text{CuSO}_4 \cdot 5\text{H}_2\text{O}$; Cu^2 , sufficiency, 50 $\mu\text{g/L}$ $\text{CuSO}_4 \cdot 5\text{H}_2\text{O}$. Scale bars = 1 cm. (b–e) The expression levels of ZmmiR398b, ZmCSD2, ZmCSD4, and ZmCSD9 in hydroponic maize plants with different Cu concentrations at 3, 5, 7, and 9 dpi, respectively. (f, g) Accumulation of SCMV RNA and coat protein (CP) in the first systemically infected leaves of hydroponic plants determined by reverse transcription-quantitative PCR and western blot assays at 3, 5, 7, and 9 dpi, respectively. CBB, Coomassie brilliant blue loading control. The results are expressed as the mean \pm SD ($n=9$), and one-way analysis of variance and Duncan's multiple comparison test were used to determine the statistical significance between the two different treatments. Different letters show statistically significant differences between treatments ($p < 0.05$).

regulating its target genes, CSDs (Leng et al., 2017). Under Cu-deficient conditions, *Arabidopsis* miR398 downregulated the expression of target genes *CSD1* and *CSD2* to regulate Cu homeostasis (Yamasaki et al., 2007). In this study, the expression levels of *Zm*miR398b were significantly increased, while the expression levels of *ZmCSD2*, *ZmCSD4*, and *ZmCSD9* were significantly decreased and promoted SCMV infection under Cu deficiency and vice versa (Figure 5). Therefore, an appropriate increase of Cu concentration can inhibit SCMV infection and improve the resistance of maize to SCMV. However, whether higher than a certain concentration of Cu will cause heavy metal stress to maize needs to be further studied.

In the present study, we characterized the *Zm*miR398b-*ZmCSD2/4/9* module that confers maize resistance to SCMV infection, probably by regulating ROS levels. Notably, Cu sufficiency

inhibited SCMV infection mainly by regulating the expression level of *Zm*miR398b-*ZmCSD2/4/9* module. We summarize this maize defence response to SCMV infection conferred by the *Zm*miR398b-*ZmCSD2/4/9* module in Figure 6.

4 | EXPERIMENTAL PROCEDURES

4.1 | Plant growth and virus inoculation

N. benthamiana plants were grown in a greenhouse (24°C, 14h/10h, day/night). Maize (*Zea mays*) inbred lines Chang7-2 and Mo17 and transgenic B104 lines were grown in growth chambers (28°C/22°C, 16h/8h, day/night). SCMV crude extracts were prepared and inoculated on the first true leaves of 1-week-old maize

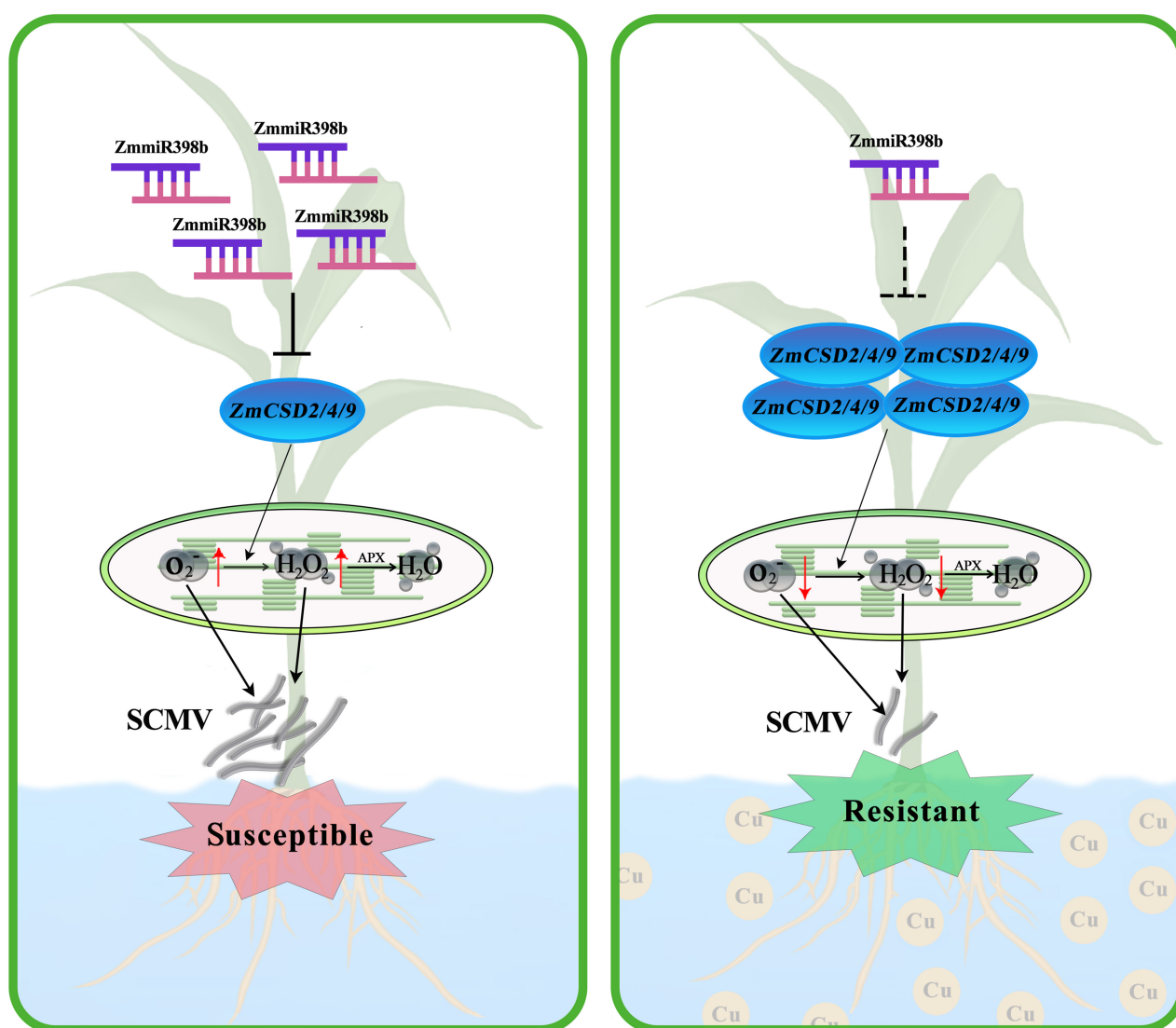


FIGURE 6 Working model of *Zm*miR398b-*ZmCSD2/4/9* module functions in maize resistance to sugarcane mosaic virus (SCMV) infection. In transgenic maize plants overexpressing *Zm*miR398b, consistent with Cu deficiency, the expression levels of *ZmCSD2/4/9* are inhibited and the content of reactive oxygen species (ROS) is increased, which is conducive to SCMV infection. In contrast, silencing *Zm*miR398b, similar to Cu sufficiency, induces the accumulation of *ZmCSD2/4/9* and reduces the ROS content, resulting in enhanced resistance to SCMV infection in maize. Arrows indicate positive regulation, and blunt-ended bars indicate inhibition.

seedlings as described previously (Gao et al., 2021). The first systemically infected leaves were harvested to determine the accumulations of ZmmiR398b, *ZmCSD2*, *ZmCSD4*, *ZmCSD9*, and SCMV RNA and CP.

4.2 | Generation of transgenic maize plants

STTM technology was used to silence ZmmiR398b according to the previous report (Yan et al., 2012). The fragment of STTM398b was obtained using the 48 nucleotides as template and STTM398b-F and STTM398b-R as primers. The *OsMIR528* precursor was selected as the backbone to produce artificial polycistronic miRNA to overexpress ZmmiR398b as described previously (Li, Chung, et al., 2013; Warthmann et al., 2008). The STTM398b and OE398b plasmids were confirmed by Sanger sequencing. The STTM398b and OE398b fragments were inserted downstream of the *UBI* promoter in the pBWA(v)BU vector. The STTM398b and OE398b recombinant vectors were introduced into *Agrobacterium tumefaciens* EHA105 and then transformed into maize inbred line B104. The *bar* gene was used for screening the genotype of transgenic plants. Details of the primers used for constructing vectors are listed in Table S1.

4.3 | Agrobacteria-mediated transient co-expression assays

The sequences of predicted target sites in *ZmCSD2*, *ZmCSD4*, and *ZmCSD9* were fused to the C-terminal of GFP and cloned into the BglII/PstI site of the binary vector pGD (Goodin et al., 2002), producing pGD-CSD2_{ts}-GFP, pGD-CSD4_{ts}-GFP, and pGD-CSD9_{ts}-GFP vectors, respectively. The ZmmiR398b-insensitive versions of pGD-CSD2_{mts}-GFP, pGD-CSD4_{mts}-GFP, and pGD-CSD9_{mts}-GFP were generated by site-directed mutagenesis using a Fast MultiSite Mutagenesis System (TransGen Biotech). The polycistronic artificial miR398b (amiR398b) that could recognize *ZmCSD2*, *ZmCSD4*, and *ZmCSD9* was amplified with primers miR398b-Bgl II-F and miR398b-Pst I-R, which was then cloned into the BglII/PstI site of the binary vector pGD, resulting in the vector pGD-miR398b. Polycistronic amiR159a was also cloned into the binary vector pGD similarly, resulting in the pGD-miR159a as a control. *A. tumefaciens* GV3101 was used for transient expression of different constructs in *N. benthamiana*. In brief, *A. tumefaciens* GV3101 harbouring different plasmids (pGD-CSD2_{ts}-GFP, pGD-CSD4_{ts}-GFP, pGD-CSD9_{ts}-GFP, pGD-CSD2_{mts}-GFP, pGD-CSD4_{mts}-GFP, pGD-CSD9_{mts}-GFP, pGD-miR398b, and pGD-miR159a) was incubated at 28°C for 14 h in liquid Luria-Bertani (LB) medium on a table shaking at 180 rpm. The *A. tumefaciens* cells were collected and resuspended in MMA buffer (10 mM MES, 10 mM MgCl₂, and 200 μM acetosyringone) until the final concentration of bacteria containing pGD-CSD2_{ts}-GFP, pGD-CSD4_{ts}-GFP, pGD-CSD9_{ts}-GFP, pGD-CSD2_{mts}-GFP, pGD-CSD4_{mts}-GFP, and pGD-CSD9_{mts}-GFP had an optical density (OD)₆₀₀ of 0.1, and pGD-miR398b, pGD-miR159a was OD₆₀₀=0, 0.1, 0.2, and 0.4, respectively. Subsequently, the mixture

containing the expression constructs was infiltrated into *N. benthamiana* leaves for transient expression assays. Laser scanning confocal microscope (Nikon) was used for image acquisition at 48 h after infiltration. Meanwhile, the infiltrated leaves were sampled to determine the expression of GFP.

4.4 | Silencing ZmCSD2/4/9 by VIGS technology

The CMV-based VIGS assays were conducted as described previously (Wang et al., 2016). Briefly, a 209-bp fragment that can target the conserved region of *ZmCSD2*, *ZmCSD4*, and *ZmCSD9* was amplified using specific primers (Table S1). The obtained fragment was subsequently cloned into pCMV201-2b_{N81} vector (KpnI/XbaI), resulting in the pCMV201-ZmCSD2/4/9 vector. Before infiltration, suspensions of *A. tumefaciens* C58C1 cells with OD₆₀₀=1.0 containing pCMV101, pCMV301, and pCMV201-ZmCSD2/4/9, were mixed in equal volumes. *A. tumefaciens* C58C1 containing pCMV201-GFP₂₅₄ was used as a control. The prepared *A. tumefaciens* suspensions were infiltrated into *N. benthamiana* leaves that were then collected after 4 days as the virus source to inject seeds of maize inbred line B73, which were grown in growth chambers (20°C/18°C, 16 h/8 h, day/night). The first true leaves of the gene-silenced maize plants were challenged by inoculation with SCMV. At 7 dpi, the expression levels of *ZmCSD2/4/9* and SCMV accumulation in the first systemically infected leaves were examined.

4.5 | Hydroponic treatments

For hydroponics experiments, the pretreatment and germination of maize inbred line Mo17 seeds were carried out according to a previous report (Sun et al., 2018). Subsequently, maize seedlings were cultured in half-strength Hoagland's nutrient solution for 2 days and full-strength Hoagland's nutrient solution with 0, 25, or 50 μg/L CuSO₄·5H₂O thereafter. The other components of the hydroponic solutions were the same as in a previous report (Du et al., 2018). The hydroponic solution was replaced every 2 days. To prevent Cu contamination in the Cu-deprived experimental set, all tools used in the hydroponic system were plastic. In the Cu-gradient hydroponic system, the first true leaves of Mo17 maize seedlings at the three-leaf stage were mechanically inoculated with SCMV. At 3, 5, 7, and 9 dpi, the first systemically infected leaves were harvested to measure the accumulations of ZmmiR398b, *ZmCSD2/4/9*, and SCMV.

4.6 | H₂O₂ and O₂⁻ visualization and determination

O₂⁻ and H₂O₂ detection in maize leaves were performed individually using NBT and DAB staining as described previously (Jabs et al., 1996; Thordal-Christensen et al., 1997) with minor modifications. In brief, the maize leaves were incubated in DAB solution (Coolaber) and NBT (Coolaber) at 37°C in the dark for 16 h. Then, the

samples were washed with 95% ethanol in boiling water for 20 min until the green colour of chlorophyll disappeared to take pictures.

4.7 | RT-qPCR analysis

The RT-qPCR assay was performed to determine the expression levels of mRNAs and miRNAs using SYBR Green PCR Master Mix (Vazyme) and a miRcute Plus miRNA qPCR Kit (Tiangen), respectively. The relative gene expression levels were calculated by the $2^{-\Delta\Delta Ct}$ method (Scheefe et al., 2006) using the mean \pm SD ($n=9$), and one-way analysis of variance and Duncan's multiple comparison test were used to determine the statistical significance between the two different treatments. The *ZmUBI* (XM_008647047) and *U6* gene (Kong et al., 2014) were used as internal controls, respectively. All primers are listed in Table S1.

4.8 | Western blot analysis

Total protein was extracted with a Plant Protein Extraction Kit (Beyotime) and quantified with a bicinchoninic acid (BCA) Protein Assay Kit (Beyotime). The total proteins were then separated by 12% SDS-PAGE gel and transferred to 0.20 μ m polyvinylidene fluoride (PVDF) membranes. Subsequently, the membranes were incubated with antibodies against GFP (1/5000, ABclonal) or SCMV CP (1/5000 dilution, LV BAO), followed by the goat antimouse IgG horseradish peroxidase (HRP) secondary antibody (1/5000 dilution, ABclonal). Finally, the membranes were transferred to the chemiluminescent substrate CDP-Star solution (Roche), and the results were visualized on a Tanon 5200 chemical luminous imaging system.

ACKNOWLEDGEMENTS

We gratefully acknowledge Professor Zaifeng Fan (China Agricultural University, Beijing) for providing the source of SCMV, Professor Tao Zhou (China Agricultural University, Beijing) for providing the CMV-VIGS vector, and Andrew O. Jackson (University of California, Berkeley, CA, USA) for providing the pGD vector. This research was supported by grants from the China Postdoctoral Science Foundation (2019M651148) and the National Natural Science Foundation of China (31801702).

CONFLICT OF INTEREST STATEMENT

The authors declare no conflict of interest.

DATA AVAILABILITY STATEMENT

The data that support the findings of this study are available from the corresponding author upon reasonable request.

ORCID

Zihao Xia  <https://orcid.org/0000-0001-7905-106X>

Yuanhua Wu  <https://orcid.org/0000-0002-8599-8679>

REFERENCES

- Abdel-Ghany, S.E. & Pilon, M. (2008) MicroRNA-mediated systemic down-regulation of copper protein expression in response to low copper availability in *Arabidopsis*. *Journal of Biological Chemistry*, 283, 15932–15945.
- Asada, K. (2006) Production and scavenging of reactive oxygen species in chloroplasts and their functions. *Plant Physiology*, 141, 391–396.
- Baldrich, P. & San Segundo, B. (2016) MicroRNAs in rice innate immunity. *Rice*, 9, 6.
- Burkhead, J.L., Gogolin Reynolds, K.A., Abdel-Ghany, S.E., Cohu, C.M. & Pilon, M. (2009) Copper homeostasis. *New Phytologist*, 182, 799–816.
- Candar-Cakir, B., Arican, E. & Zhang, B. (2016) Small RNA and degradome deep sequencing reveals drought-and tissue-specific microRNAs and their important roles in drought-sensitive and drought-tolerant tomato genotypes. *Plant Biotechnology Journal*, 14, 1727–1746.
- Chaudhary, S., Grover, A. & Sharma, P.C. (2021) MicroRNAs: potential targets for developing stress-tolerant crops. *Life*, 11, 289.
- Chen, X. (2004) A microRNA as a translational repressor of *APETALA2* in *Arabidopsis* flower development. *Science*, 303, 2022–2025.
- Cui, C., Wang, J.J., Zhao, J.H., Fang, Y.Y., He, X.F., Guo, H.S. et al. (2020) A *Brassica* miRNA regulates plant growth and immunity through distinct modes of action. *Molecular Plant*, 13, 231–245.
- Dong, Q., Hu, B. & Zhang, C. (2022) microRNAs and their roles in plant development. *Frontiers in Plant Science*, 13, 824240.
- Du, Q., Wang, K., Zou, C., Xu, C. & Li, W.X. (2018) The *PILNCR1*-miR399 regulatory module is important for low phosphate tolerance in maize. *Plant Physiology*, 177, 1743–1753.
- Fan, Z.F., Chen, H.Y., Liang, X.M. & Li, H.F. (2003) Complete sequence of the genomic RNA of the prevalent strain of a potyvirus infecting maize in China. *Archives of Virology*, 148, 773–782.
- Gao, X., Chen, Y., Luo, X., Du, Z., Hao, K., An, M. et al. (2021) Recombinase polymerase amplification assay for simultaneous detection of maize chlorotic mottle virus and sugarcane mosaic virus in maize. *ACS Omega*, 6, 18008–18013.
- Gao, X., Hao, K., Du, Z., Zhang, S., Guo, J., Li, J. et al. (2023) Whole-transcriptome characterization and functional analysis of lncRNA-miRNA-mRNA regulatory networks responsive to sugarcane mosaic virus in maize resistant and susceptible inbred lines. *International Journal of Biological Macromolecules*, 257, 128685.
- Gill, S.S. & Tuteja, N. (2010) Reactive oxygen species and antioxidant machinery in abiotic stress tolerance in crop plants. *Plant Physiology and Biochemistry*, 48, 909–930.
- Goodin, M.M., Dietzgen, R.G., Schichnes, D., Ruzin, S. & Jackson, A.O. (2002) pGD vectors: versatile tools for the expression of green and red fluorescent protein fusions in agroinfiltrated plant leaves. *The Plant Journal*, 31, 375–383.
- Guan, Q., Lu, X., Zeng, H., Zhang, Y. & Zhu, J. (2013) Heat stress induction of *miR398* triggers a regulatory loop that is critical for thermotolerance in *Arabidopsis*. *The Plant Journal*, 74, 840–851.
- Guo, H.S., Xie, Q., Fei, J.F. & Chua, N.H. (2005) MicroRNA directs mRNA cleavage of the transcription factor *NAC1* to downregulate auxin signals for *Arabidopsis* lateral root development. *The Plant Cell*, 17, 1376–1386.
- Jabs, T., Dietrich, R.A. & Dangl, J.L. (1996) Initiation of runaway cell death in an *Arabidopsis* mutant by extracellular superoxide. *Science*, 273, 1853–1856.
- Jajic, I., Sarna, T. & Strzalka, K. (2015) Senescence, stress, and reactive oxygen species. *Plants*, 4, 393–411.
- Jiang, J.X. & Zhou, X.P. (2002) Maize dwarf mosaic disease in different regions of China is caused by *Sugarcane mosaic virus*. *Archives of Virology*, 147, 2437–2443.
- Jiang, T., Du, K., Wang, P., Wang, X., Zang, L., Peng, D. et al. (2022) Sugarcane mosaic virus orchestrates the lactate fermentation

- pathway to support its successful infection. *Frontiers in Plant Science*, 13, 1099362.
- Jiao, Z., Tian, Y., Cao, Y., Wang, J., Zhan, B., Zhao, Z. et al. (2021) A novel pathogenicity determinant hijacks maize catalase 1 to enhance viral multiplication and infection. *New Phytologist*, 230, 1126–1141.
- Jiao, Z., Tian, Y., Wang, J., Ismail, R.G., Bondok, A. & Fan, Z. (2022) Advances in research on maize lethal necrosis, a devastating viral disease. *Phytopathology Research*, 4, 14.
- Kasschau, K.D., Xie, Z., Allen, E., Llave, C., Chapman, E.J., Krizan, K.A. et al. (2003) P1/HC-Pro, a viral suppressor of RNA silencing, interferes with *Arabidopsis* development and miRNA function. *Developmental Cell*, 4, 205–217.
- Kaur, N., Dhawan, M., Sharma, I. & Pati, P.K. (2016) Interdependency of reactive oxygen species generating and scavenging system in salt sensitive and salt tolerant cultivars of rice. *BMC Plant Biology*, 16, 131.
- Kong, X., Zhang, M., Xu, X., Li, X., Li, C. & Ding, Z. (2014) System analysis of microRNAs in the development and aluminium stress responses of the maize root system. *Plant Biotechnology Journal*, 12, 1108–1121.
- Lei, R., Du, Z., Qiu, Y. & Zhu, S. (2016) The detection of hydrogen peroxide involved in plant virus infection by fluorescence spectroscopy. *Luminescence*, 31, 1158–1165.
- Leng, X., Wang, P., Zhu, X., Li, X., Zheng, T., Shangguan, L. et al. (2017) Ectopic expression of *CSD1* and *CSD2* targeting genes of miR398 in grapevine is associated with oxidative stress tolerance. *Functional & Integrative Genomics*, 17, 697–710.
- Li, J., Guo, G., Guo, W., Guo, G., Tong, D., Ni, Z. et al. (2012) miRNA164-directed cleavage of *ZmNAC1* confers lateral root development in maize (*Zea mays* L.). *BMC Plant Biology*, 12, 220.
- Li, J.F., Chung, H.S., Niu, Y., Bush, J., McCormack, M. & Sheen, J. (2013) Comprehensive protein-based artificial microRNA screens for effective gene silencing in plants. *The Plant Cell*, 25, 1507–1522.
- Li, Y., Cao, X.L., Zhu, Y., Yang, X.M., Zhang, K.N., Xiao, Z.Y. et al. (2019) Osa-miR398b boosts H₂O₂ production and rice blast disease-resistance via multiple superoxide dismutases. *New Phytologist*, 222, 1507–1522.
- Li, Y., Liu, R., Zhou, T. & Fan, Z. (2013) Genetic diversity and population structure of *Sugarcane mosaic virus*. *Virus Research*, 171, 242–246.
- Li, Y., Lu, Y.G., Shi, Y., Wu, L., Xu, Y.J., Huang, F. et al. (2014) Multiple rice microRNAs are involved in immunity against the blast fungus *Magnaporthe oryzae*. *Plant Physiology*, 164, 1077–1092.
- Lin, K.Y., Wu, S.Y., Hsu, Y.H. & Lin, N.S. (2022) miR398-regulated antioxidants contribute to *Bamboo mosaic virus* accumulation and symptom manifestation. *Plant Physiology*, 188, 593–607.
- Liu, J., Fan, H., Wang, Y., Han, C., Wang, X., Yu, J. et al. (2020) Genome-wide microRNA profiling using oligonucleotide microarray reveals regulatory networks of microRNAs in *Nicotiana benthamiana* during beet necrotic yellow vein virus infection. *Viruses*, 12, 310.
- Liu, Q., Deng, S., Liu, B., Tao, Y., Ai, H., Liu, J. et al. (2020) A *helitron*-induced RabGDI α variant causes quantitative recessive resistance to maize rough dwarf disease. *Nature Communications*, 11, 495.
- Liu, X., Liu, S., Chen, X., Prasanna, B.M., Ni, Z., Li, X. et al. (2022) Maize miR167-ARF3/30-polyamine oxidase 1 module-regulated H₂O₂ production confers resistance to maize chlorotic mottle virus. *Plant Physiology*, 189, 1065–1082.
- Liu, Y., Yu, Y., Fei, S., Chen, Y., Xu, Y., Zhu, Z. et al. (2023) Overexpression of sly-miR398b compromises disease resistance against *Botrytis cinerea* through regulating ROS homeostasis and JA-related defense genes in tomato. *Plants*, 12, 2572.
- Lu, Q., Guo, F., Xu, Q. & Cang, J. (2020) lncRNA improves cold resistance of winter wheat by interacting with miR398. *Functional Plant Biology*, 47, 544–557.
- Mahuku, G., Lockhart, B.E., Wanjala, B., Jones, M.W., Kimunye, J.N., Stewart, L.R. et al. (2015) Maize lethal necrosis (MLN), an emerging threat to maize-based food security in sub-Saharan Africa. *Phytopathology*, 105, 956–965.
- Mhamdi, A. & Van Breusegem, F. (2018) Reactive oxygen species in plant development. *Development*, 145, dev164376.
- Mittler, R. (2002) Oxidative stress, antioxidants and stress tolerance. *Trends in Plant Science*, 7, 405–410.
- Pacheco, R., García-Marcos, A., Barajas, D., Martiáñez, J. & Tenllado, F. (2012) PVX-potyvirus synergistic infections differentially alter microRNA accumulation in *Nicotiana benthamiana*. *Virus Research*, 165, 231–235.
- Padmanabhan, C., Zhang, X. & Jin, H. (2009) Host small RNAs are big contributors to plant innate immunity. *Current Opinion in Plant Biology*, 12, 465–472.
- Pilon, M. (2017) The copper microRNAs. *New Phytologist*, 213, 1030–1035.
- Quan, L.J., Zhang, B., Shi, W.W. & Li, H.Y. (2008) Hydrogen peroxide in plants: a versatile molecule of the reactive oxygen species network. *Journal of Integrative Plant Biology*, 50, 2–18.
- Racchi, M.L. (2013) Antioxidant defenses in plants with attention to *Prunus* and *Citrus* spp. *Antioxidants*, 2, 340–369.
- Redinbaugh, M.G. & Stewart, L.R. (2018) Maize lethal necrosis: an emerging, synergistic viral disease. *Annual Review of Virology*, 5, 301–322.
- Saxena, I., Srikanth, S. & Chen, Z. (2016) Cross talk between H₂O₂ and interacting signal molecules under plant stress response. *Frontiers in Plant Science*, 7, 570.
- Scheffe, J.H., Lehmann, K.E., Buschmann, I.R., Unger, T. & Funke-Kaiser, H. (2006) Quantitative real-time RT-PCR data analysis: current concepts and the novel “gene expression's C_T difference” formula. *Journal of Molecular Medicine*, 84, 901–910.
- Shi, C., Ingvarsdén, C., Thümmler, F., Melchinger, A.E., Wenzel, G. & Lübberstedt, T. (2005) Identification by suppression subtractive hybridization of genes that are differentially expressed between near-isogenic maize lines in association with sugarcane mosaic virus resistance. *Molecular Genetics and Genomics*, 273, 450–461.
- Shukla, D.D., Tomic, M., Jilka, J., Ford, R.E., Toler, R.W. & Langham, M.A.C.J.P. (1989) Taxonomy of potyviruses infecting maize, sorghum, and sugarcane in Australia and the United States as determined by reactivities of polyclonal antibodies directed towards virus-specific N-termini of coat proteins. *Phytopathology*, 79, 223–229.
- Sun, Q., Liu, X., Yang, J., Liu, W., Du, Q., Wang, H. et al. (2018) MicroRNA528 affects lodging resistance of maize by regulating lignin biosynthesis under nitrogen-luxury conditions. *Molecular Plant*, 11, 806–814.
- Sun, Z., Shu, L., Zhang, W. & Wang, Z. (2020) Cca-miR398 increases copper sulfate stress sensitivity via the regulation of *CSD* mRNA transcription levels in transgenic *Arabidopsis thaliana*. *PeerJ*, 8, e9105.
- Sunkar, R., Kapoor, A. & Zhu, J.K. (2006) Posttranscriptional induction of two Cu/Zn superoxide dismutase genes in *Arabidopsis* is mediated by downregulation of miR398 and important for oxidative stress tolerance. *The Plant Cell*, 18, 2051–2065.
- Sunkar, R. & Zhu, J.K. (2004) Novel and stress-regulated microRNAs and other small RNAs from *Arabidopsis*. *The Plant Cell*, 16, 2001–2019.
- Suzuki, T., Ikeda, S., Kasai, A., Taneda, A., Fujibayashi, M., Sugawara, K. et al. (2019) RNAi-mediated down-regulation of Dicer-Like 2 and 4 changes the response of ‘Moneymaker’ tomato to potato spindle tuber viroid infection from tolerance to lethal systemic necrosis, accompanied by up-regulation of miR398, 398a-3p and production of excessive amount of reactive oxygen species. *Viruses*, 11, 344.
- Tang, J. & Chu, C. (2017) MicroRNAs in crop improvement: fine-tuners for complex traits. *Nature Plants*, 3, 17077.
- Thordal-Christensen, H., Zhang, Z., Wei, Y. & Collinge, D.B.J.T.P.J. (1997) Subcellular location of H₂O₂ in plants: H₂O₂ accumulation in papillae and hypersensitive response during the barley-powdery mildew interaction. *The Plant Journal*, 11, 1187–1194.
- Tian, Y., Jiao, Z., Qi, F., Ma, W., Hao, Y., Wang, X. et al. (2024) Maize catalases are recruited by a virus to modulate viral multiplication and infection. *Molecular Plant Pathology*, 25, e13440.
- Wang, J., Mei, J. & Ren, G. (2019) Plant microRNAs: biogenesis, homeostasis, and degradation. *Frontiers in Plant Science*, 10, 360.

- Wang, R., Yang, X., Wang, N., Liu, X., Nelson, R.S., Li, W. et al. (2016) An efficient virus-induced gene silencing vector for maize functional genomics research. *The Plant Journal*, 86, 102–115.
- Warthmann, N., Chen, H., Ossowski, S., Weigel, D. & Hervé, P. (2008) Highly specific gene silencing by artificial miRNAs in rice. *PLoS One*, 3, e1829.
- Waszczak, C., Carmody, M. & Kangasjärvi, J. (2018) Reactive oxygen species in plant signaling. *Annual Review of Plant Biology*, 69, 209–236.
- Wu, J., Yang, R., Yang, Z., Yao, S., Zhao, S., Wang, Y. et al. (2017) ROS accumulation and antiviral defence control by microRNA528 in rice. *Nature Plants*, 3, 16203.
- Xia, Z., Zhao, Z., Li, M., Chen, L., Jiao, Z., Wu, Y. et al. (2018) Identification of miRNAs and their targets in maize in response to Sugarcane mosaic virus infection. *Plant Physiology and Biochemistry*, 125, 143–152.
- Xin, M., Wang, Y., Yao, Y., Xie, C., Peng, H., Ni, Z. et al. (2010) Diverse set of microRNAs are responsive to powdery mildew infection and heat stress in wheat (*Triticum aestivum* L.). *BMC Plant Biology*, 10, 123.
- Xu, W., Meng, Y. & Wise, R.P. (2014) *Mla*- and *Rom1*-mediated control of microRNA398 and chloroplast copper/zinc superoxide dismutase regulates cell death in response to the barley powdery mildew fungus. *New Phytologist*, 201, 1396–1412.
- Yamasaki, H., Abdel-Ghany, S.E., Cohu, C.M., Kobayashi, Y., Shikanai, T. & Pilon, M. (2007) Regulation of copper homeostasis by micro-RNA in *Arabidopsis*. *Journal of Biological Chemistry*, 282, 16369–16378.
- Yamasaki, H., Pilon, M. & Shikanai, T. (2008) How do plants respond to copper deficiency? *Plant Signaling & Behavior*, 3, 231–232.
- Yan, J., Gu, Y., Jia, X., Kang, W., Pan, S., Tang, X. et al. (2012) Effective small RNA destruction by the expression of a short tandem target mimic in *Arabidopsis*. *The Plant Cell*, 24, 415–427.
- Yao, S., Kang, J., Guo, G., Yang, Z., Huang, Y., Lan, Y. et al. (2022) The key micronutrient copper orchestrates broad-spectrum virus resistance in rice. *Science Advances*, 8, eabm0660.
- Yu, X., Wang, H., Lu, Y., de Ruiter, M., Cariaso, M., Prins, M. et al. (2012) Identification of conserved and novel microRNAs that are responsive to heat stress in *Brassica rapa*. *Journal of Experimental Botany*, 63, 1025–1038.
- Zhang, C., Ding, Z., Wu, K., Yang, L., Li, Y., Yang, Z. et al. (2016) Suppression of jasmonic acid-mediated defense by viral-inducible microRNA319 facilitates virus infection in rice. *Molecular Plant*, 9, 1302–1314.
- Zhang, X., Du, P., Lu, L., Xiao, Q., Wang, W., Cao, X. et al. (2008) Contrasting effects of HC-Pro and 2b viral suppressors from *Sugarcane mosaic virus* and *Tomato aspermy cucumovirus* on the accumulation of siRNAs. *Virology*, 374, 351–360.
- Zhu, F., Cao, M.Y., Zhu, P.X., Zhang, Q.P. & Lam, H.M. (2023) Non-specific LIPID TRANSFER PROTEIN 1 enhances immunity against tobacco mosaic virus in *Nicotiana benthamiana*. *Journal of Experimental Botany*, 74, 5236–5254.

SUPPORTING INFORMATION

Additional supporting information can be found online in the Supporting Information section at the end of this article.

How to cite this article: Gao, X., Du, Z., Hao, K., Zhang, S., Li, J., Guo, J. et al. (2024) ZmmiR398b negatively regulates maize resistance to sugarcane mosaic virus infection by targeting *ZmCSD2/4/9*. *Molecular Plant Pathology*, 25, e13462. Available from: <https://doi.org/10.1111/mpp.13462>